BMC Medical Imaging

RESEARCH

Open Access

A non-invasive preoperative model for predicting sentinel lymph node metastasis in breast cancer using clinical data and MRI

Yunqing Yang[1], Zhulin Wang[2], Haidong Wang[3], Yun Wang[4] and Yang Fu[5*]

Abstract

Introduction Breast cancer is the leading cause of cancer-related death among women, with metastasis accounting for the majority of these deaths. Sentinel lymph node (SLN) status is crucial for staging and treatment planning. This study aims to develop a non-invasive preoperative model for predicting SLN metastasis using clinical data and preoperative MRI.

Methods A retrospective study included 4,276 breast cancer patients who underwent surgery were enrolled. After exclusions, 999 patients were analyzed. Univariable and multivariable logistic regression identified significant predictors of SLN metastasis, which were used to construct nomograms. Calibration curves and decision curve analysis (DCA) validated the model's accuracy. Recursive partitioning analysis (RPA) was used to create a risk stratification system.

Results Significant predictors of SLN metastasis included tumor size on MRI, multifocality, MRI-BIRADS classification, ADC value, short axis, and cortical thickness ($P < 0.05$). The nomogram showed excellent discriminatory power with an AUC of 0.847. The RPA stratified patients into low-, intermediate-, and high-risk groups, with respective SLN metastasis probabilities of 15.8%, 28.6%, and 69.8%.

Conclusions This non-invasive SLN metastasis prediction model and risk stratification system provide a valuable tool for personalized clinical decision-making, potentially reducing the need for SLN biopsy in low-risk patients. Further studies are needed to validate these findings.

Keywords Breast cancer, Sentinel lymph node, Dynamic contrast-enhanced MRI (DCE-MRI), Nomogram, Decision curve analysis, Recursive partitioning analysis

*Correspondence:
Yang Fu
fuyang@zzu.edu.cn
[1]Department of Breast Surgery, The First Affiliated Hospital of Zhengzhou University, Zhengzhou, Henan Province, China
[2]Department of Thoracic Surgery, Affiliated Hospital of Southwest Medical University, Luzhou, Sichuan Province, China
[3]Department of General Surgery, Anyang Dengta Hospital, Anyang, Henan Province, China
[4]Department of Magnetic Resonance Imaging, The First Affiliated Hospital of Zhengzhou University, Zhengzhou, Henan Province, China
[5]Department of Gastrointestinal Surgery, The First Affiliated Hospital of Zhengzhou University, Zhengzhou 450052, China

Introduction

The incidence of female breast cancer has increased by approximately 0.5% annually since the mid-2000s [1]. Currently, breast cancer is the most commonly diagnosed malignant disease among women, accounting for 31% of all newly diagnosed cancers [2]. The status of axillary lymph nodes (ALN) is a critical factor in determining prognosis and developing individualized treatment plans. However, axillary lymph node dissection (ALND) has been associated with numerous postoperative complications, such as reduced range of motion, arm and shoulder pain, and lymphedema [3, 4]. Although sentinel lymph node biopsy (SLNB) is less invasive with fewer complications than ALND, it can still lead to shoulder dysfunction, paralysis, and lymphedema, diminishing patients' quality of life. Moreover, the false-negative rate of SLNB is 5.5% [5]. Additionally, prolonged intraoperative pathology waiting times result in extended anesthesia duration, increased costs, and heightened risk of postoperative venous thrombosis. As such, non-invasive examination of SLN metastasis has become a critical focus in clinical practice.

Further clarification of imaging criteria is needed for assessing lymph node metastasis. While lymph nodes with a diameter exceeding 1 cm are classified as metastatic, many nodes smaller than 1 cm are malignant, and larger nodes are often benign due to inflammatory conditions [6]. Liu et al. [7] proposed using a long-to-short axis diameter ratio of less than 1.52 to predict lymph node metastasis. Similarly, Kim et al. [8] utilized lymph node characteristics such as long and short axes and cortical thickness to forecast ALN metastasis.

Numerous attempts have been undertaken to develop predictive models for SLN metastasis in breast cancer. However, some models rely on postoperative pathological data unavailable preoperatively or on advanced technologies like machine learning and artificial intelligence, which are difficult to implement widely. To address these limitations, this study combined clinical data with preoperative MRI images to develop a non-invasive model for predicting SLN metastasis. Additionally, it established a risk stratification system using recursive partitioning analysis (RPA), marking a novel contribution to this field.

Materials and methods

Patients

This retrospective study was approved by the Zhengzhou University Institutional Review Board (No. 2023-KY-0586). A total of 4,276 histologically confirmed breast cancer patients undergoing surgery at the Department of Breast Surgery, First Affiliated Hospital of Zhengzhou University, between January 2020 and September 2022, were included (Fig. 1). Exclusion criteria encompassed male breast cancer ($n=3$), ductal carcinoma in situ ($n=115$), ductal carcinoma in situ with microinvasion ($n=122$), specific invasive breast cancer ($n=41$), and cases without MRI scans ($n=2,430$). Additional exclusions involved cases without SLNB ($n=153$), surgeries conducted at other hospitals ($n=202$), patients who underwent neoadjuvant chemotherapy ($n=191$), and palliative surgeries ($n=15$). Five patients lacking postoperative pathological reports were also excluded. This resulted in 999 patients, including 992 unilateral and 7 bilateral invasive breast cancer cases, for a total of 1,006 cases.

MR image acquisition

MRI acquisition was conducted using a 3.0T scanner (GE Discovery 750 W) equipped with an 8-channel breast-dedicated coil. Patients were positioned prone with their breasts securely placed within the coil. MRI sequences included axial T1WI, axial T2WI, DCE-MRI, DWI, and sagittal contrast-enhanced imaging. Second-phase (61–122 s) DCE images, which provided optimal tumor-to-background contrast, were selected for analysis. Recorded MRI parameters comprised tumor size, ADC values, long axis, short axis, and cortical thickness of the most suspicious level Ⅰ axillary lymph node depending on morphological features according to previous reports (Fig. 2) [26]. When more than one suspicious lymph node was identified, the largest-appearing node was selected as the most suspicious level Ⅰ axillary lymph node. Measurements were initially assessed by a radiologist with 9 years of expertise and subsequently reviewed by a senior radiologist possessing over 12 years of expertise. To assess reproducibility, a subset of 32 patients was independently evaluated by two radiologists, and Interobserver agreement was assessed using the intraclass correlation coefficient (ICC, two-way random-effects model, absolute agreement). The ICC for tumor size measurements was 0.89 (95% CI: 0.83–0.94), indicating good to excellent agreement between the two radiologists. Both radiologists were blinded to the tumor's pathological type and SLN status.

Statistical analysis

Statistical analyses were conducted using SPSS (version 27) and R (version 4.1). Categorical variables were analyzed using the chi-squared test and expressed as percentages (%). Continuous variables were represented as means ± standard deviations and analyzed with the independent sample t-test. To determine optimal cutoff values for SLN metastasis prediction, receiver operating characteristic (ROC) curves of long axis, short axis, and cortical thickness measurements were generated. The Youden index was applied to establish threshold values. Univariable logistic regression identified clinically significant variables ($P<0.05$), which were subsequently

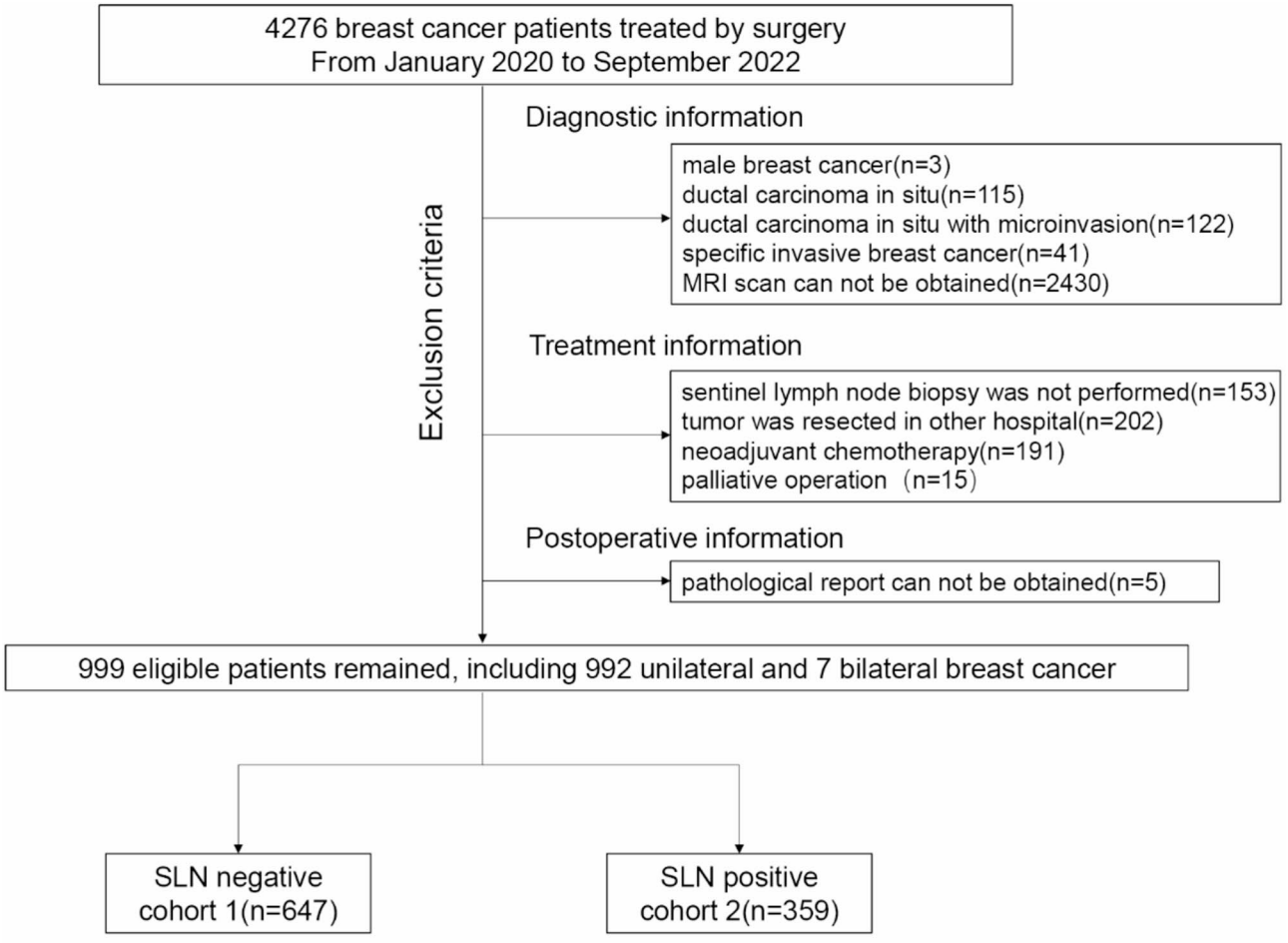

Fig. 1 Flow diagram for selection of the study cohort. SLN, sentinel lymph node

incorporated into multivariable logistic regression. A prediction nomogram was then constructed (Fig. 4).

Results

Patient characteristics

The characteristics of the study population are summarized in Table 1. The mean values for the long axis, short axis, and cortical thickness of the most suspicious level Ⅰ axillary lymph node on MRI were 10.06 ± 3.469 mm, 6.87 ± 2.131 mm, and 2.78 ± 1.278 mm, respectively. Based on the ROC curves (Fig. 3), the long axis, short axis, and cortical thickness could be potential diagnostic markers for SLN metastasis. The respective cutoff values for these parameters were 9.7 mm, 7.0 mm, and 2.7 mm (Tables 1 and 2). Table 2 summarizes additional data regarding the ROC curves.

Risk stratification of SLN metastasis

Univariable logistic analysis identified significant associations between SLN positivity and various factors, including tumor size on MRI, tumor location on MRI, multifocality, MRI-BIRADS classification, ADC value, long axis, short axis, and cortical thickness ($P < 0.05$) (Table S1). Multivariable logistic regression further revealed that tumor size on MRI, multifocality, MRI-BIRADS classification, ADC value, short axis, and cortical thickness were independently associated with SLN positivity ($P < 0.05$) (Table S2). These findings were subsequently utilized to construct prediction nomograms (Fig. 4).

The SLN nomogram demonstrated strong discriminatory power, with a concordance index of 0.847 (0.822–0.872) (Fig. 5). Calibration curves validated the agreement between observed SLN metastasis probabilities and nomogram-predicted probabilities (Figure S1). Decision curve analysis (DCA) further highlighted the model's clinical utility, with the greatest net benefit observed when the SLN metastasis probability threshold was set between 0.04 and 0.081 (Figure S2).

Recursive partitioning analysis (RPA) was employed to stratify patients by SLN metastasis risk. A two-node decision tree was constructed using cortical thickness and ADC values to classify patients into three distinct risk groups: (i) low risk (cortical thickness of the

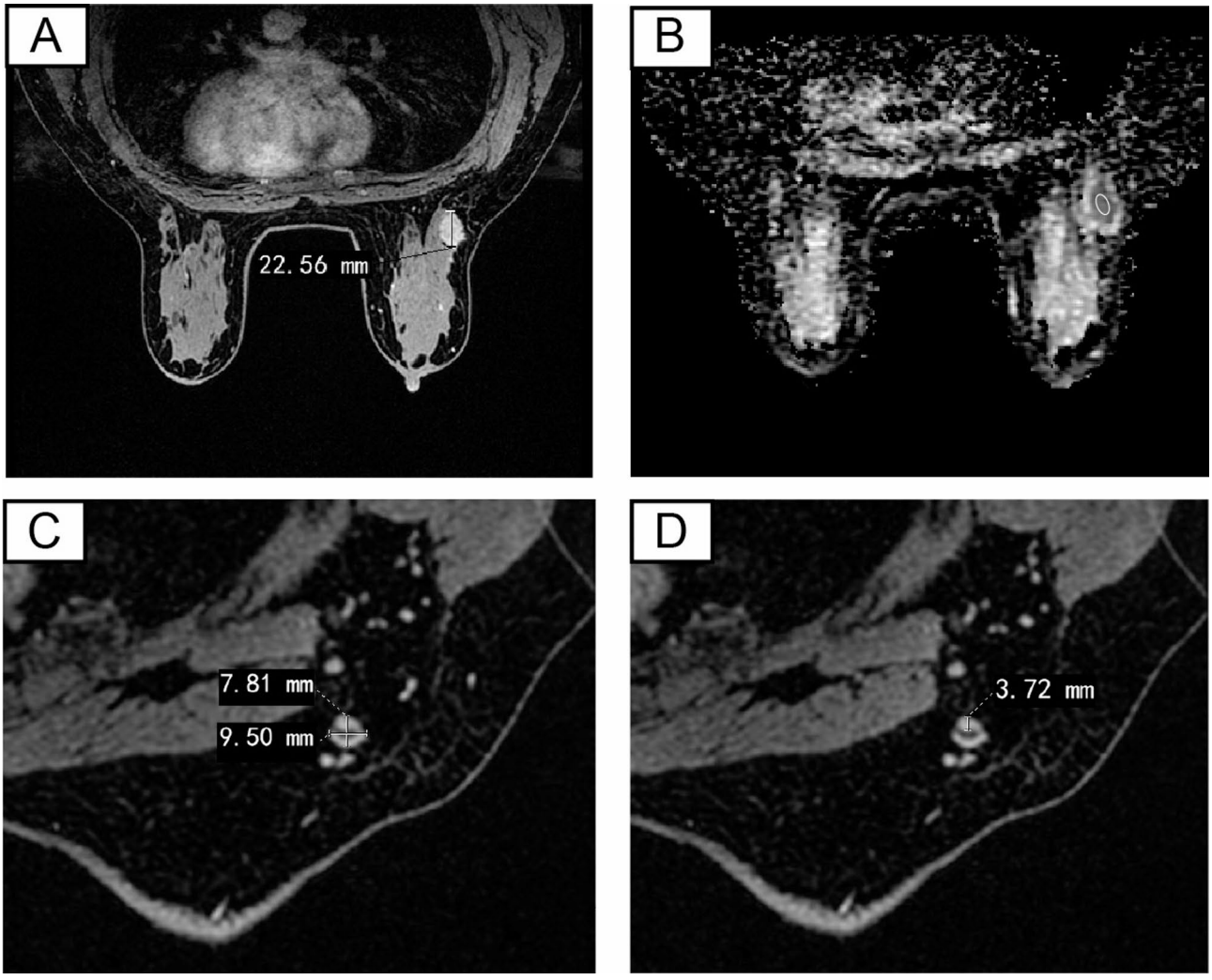

Fig. 2 Methods of measuring tumor and the most suspicious level Ⅰ axillary lymph node status on MRI. **A** The maximum diameter as tumor size. **B** The ADC value of the tumor was derived from the average of three measurements taken by the radiologist at different locations of the ROIs. **C** The maximum long diameter and the maximum short diameter of the target lymph node. **D** The maximum cortical thickness of the target lymph node. ADC, apparent diffusion coefficient; ROIs, region of interests

targeted lymph node ≤ 2.7 mm), (ii) intermediate risk (cortical thickness of the targeted lymph node > 2.7 mm and ADC ≥ 1.164×10^{-3} mm^2/s), and (iii) high risk (cortical thickness of the targeted lymph node > 2.7 mm and ADC < 1.164×10^{-3} mm^2/s). The respective risks of SLN metastasis for these groups were 15.8%, 28.6%, and 69.8% (Fig. 6).

Discussion

Axillary lymph node metastasis is a critical predictor of tumor recurrence and survival in patients with breast cancer. Accurate preoperative assessment of SLN status is vital for evaluating the N stage of breast cancer to guide clinical decision-making. While pathological examination following SLNB remains the gold standard for diagnosing SLN metastasis, non-invasive prediction methods have emerged as promising alternatives. Consequently, it is essential to investigate the risk factors associated with SLN metastasis and to develop effective risk stratification systems and preoperative prediction models.

Numerous predictive models for lymph node metastasis in breast cancer have been developed. However, these models vary widely in research factors, methodologies, and outcomes, yet lack a unified standard [9–18]. Some models rely on advanced technologies, such as radiomics, machine learning, and deep learning, which are often inaccessible in many healthcare settings, particularly at the community level. Others incorporate conventional pathological and immunohistochemical markers, which are unavailable preoperatively. This study aims to address these limitations by developing a straightforward, pragmatic, and accessible preoperative prediction model.

In this study, tumor size on MRI, multifocality, MRI-BIRADS classification, ADC value, short axis, and

Table 1 Clinical characteristics and MRI morphologic findings of patients

Variables	SLN- (*n* = 647)	SLN+ (*n* = 359)	Total (*n* = 1006)	*P*-value
Age(y), n (%)				0.476
Median (min, max)	51(27,81)	51(27,75)	51(27,81)	
< 35	30(4.6)	23(6.4)	53(5.3)	
35–50	277(42.8)	153(42.6)	430(42.7)	
> 50	340(52.6)	183(51.0)	523(52.0)	
BMI, mean ± SD	24.14 ± 2.604	24.09 ± 2.698	24.12 ± 2.637	0.754
Age of menarche(y), median (min, max)	14(10,19)	14(9,19)	14(9,19)	
Age of menopause(y), media (min, max)	50(35,61)	50(35,57)	50(35,61)	
Menopause, n (%)				0.631
No	334(51.6)	191(53.2)	525(52.2)	
Yes	313(48.4)	168(46.8)	481(47.8)	
Times of pregnancy, median (min, max)	3(0,10)	3(0,8)	3(0,10)	0.350
Times of bearing birth, median (min, max)	2(0,8)	2(0,6)	2(0,8)	0.065
Times of abortion, median (min, max)	1(0,6)	1(0,6)	1(0,6)	0.984
Tumor location, n (%)				0.362
Left breast	342(52.9)	179(49.9)	521(51.8)	
Right breast	305(47.1)	180(50.1)	485(48.2)	
Tumor size on MRI (cm), n (%)				< 0.001
mean ± SD	2.09 ± 0.998	2.58 ± 1.266	2.27 ± 1.125	
T ≤ 2	375(58.0)	134(37.3)	509(50.6)	
2 < T ≤ 5	256(39.6)	208(57.9)	464(46.1)	
T > 5	16(2.5)	17(4.7)	33(3.3)	
Tumor location on MRI, n (%)				0.015
Upper outer quadrant	234(36.2)	153(42.6)	387(38.5)	
Lower outer quadrant	144(22.3)	81(22.6)	225(22.4)	
Upper inner quadrant	169(26.1)	73(20.3)	242(24.1)	
Lower inner quadrant	66(10.2)	23(6.4)	89(8.8)	
Central quadrant	34(5.3)	29(8.1)	63(6.3)	
Multifocality, n (%)				< 0.001
No	613(94.7)	308(85.8)	921(91.6)	
Yes	34(5.3)	51(14.2)	85(8.4)	
MRI-BIRADS classification, n (%)				< 0.001
BIRADS 3	26(4.0)	3(0.8)	29(2.9)	
BIRADS 4	476(73.6)	220(61.3)	696(69.2)	
BIRADS 5	145(22.4)	136(37.9)	281(27.9)	
TIC curve type, n (%)				0.401
I	35(5.4)	27(7.5)	62(6.2)	
II	474(73.3)	255(71.0)	729(72.5)	
III	138(21.3)	77(21.4)	215(21.4)	
ADC value($\times 10^{-3} mm^2/s$), mean ± SD	0.98 ± 0.174	0.92 ± 0.143	0.96 ± 0.166	< 0.001
Long axis(mm), n (%)				< 0.001
mean ± SD	8.94 ± 2.612	12.06 ± 3.902	10.06 ± 3.469	
≤ 9.7 mm	440(68.0)	118(32.9)	558(55.5)	
> 9.7 mm	207(32.0)	241(67.1)	448(44.5)	
Short axis(mm), n (%)				< 0.001
mean ± SD	6.07 ± 1.478	8.30 ± 2.369	6.87 ± 2.131	
≤ 7.0 mm	500(77.3)	113(31.5)	613(60.9)	
> 7.0 mm	147(22.7)	246(68.5)	393(39.1)	
Cortical thickness (mm), n (%)				< 0.001
mean ± SD	2.27 ± 0.652	3.71 ± 1.575	2.78 ± 1.278	

Table 1 (continued)

Variables	SLN- (*n* = 647)	SLN+ (*n* = 359)	Total (*n* = 1006)	*P*-value
≤ 2.7 mm	517(79.9)	97(27.0)	614(61.0)	
> 2.7 mm	130(20.1)	262(73.0)	392(39.0)	0.341
Long-to-short-axis ratio, mean ± SD	1.49 ± 0.324	1.47 ± 0.321	1.48 ± 0.323	

MRI, magnetic resonance imaging; SLN, sentinel lymph node; BMI, body mass index; SD, standard deviation; TIC, time-intensity curve; ADC, apparent diffusion coefficient

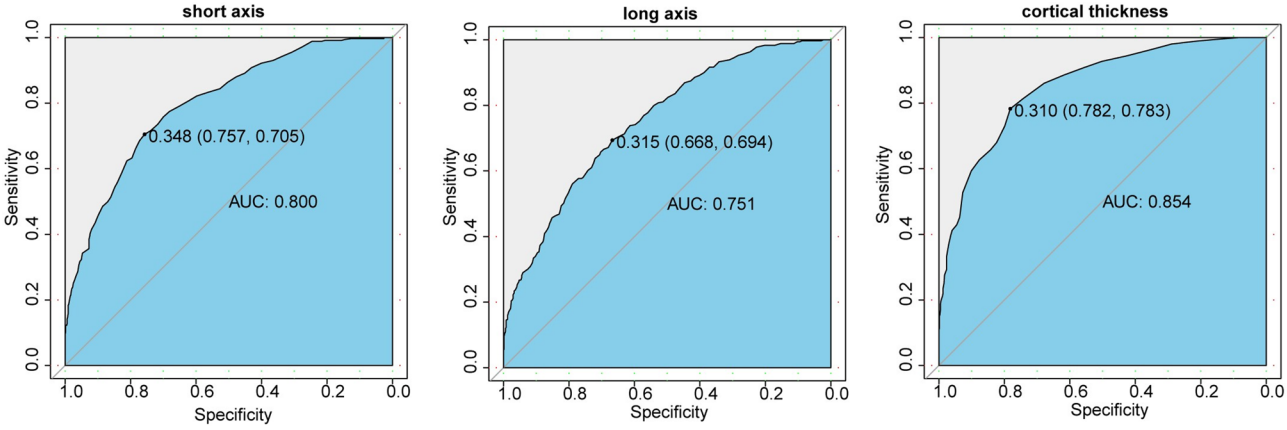

Fig. 3 The ROC curve of short axis, long axis and cortical thickness of the most suspicious level Ⅰ axillary lymph node on MRI. ROC, receiver operating characteristic; MRI, magnetic resonance imaging

Table 2 Detailed information in ROC curves of SLN metastasis

Variables	Long axis	Short axis	Cortical thickness
Cutoff value	9.7 mm	7.0 mm	2.7 mm
AUC (95% CI)	0.751 (0.721–0.782)	0.800 (0.772–0.827)	0.854 (0.830–0.878)
Sensitivity	69.4%	70.5%	78.3%
Specificity	66.8%	75.7%	78.2%
p-value	< 0.001	< 0.001	< 0.001

ROC, receiver operating characteristic; SLN, sentinel lymph node; AUC, area under the curve; CI, confidence interval

cortical thickness were significantly correlated with SLN positivity ($P < 0.05$). The probability of SLN metastasis was found to be twice as high in cases where the tumor size > 5 cm on MRI (51.5%, 17/33) compared to cases ≤ 2 cm (26.3%, 134/509). Indicatively, the potential for metastasis to SLNs escalates in correlation with the extent of the tumor. Consistent with previous reports [19–21]. In this study, the probability of SLN metastasis in single or multiple tumors was 33.4% (308/921) and 60.0% (51/85), respectively. In cases where the tumors were multifocal, the probability of SLN metastasis was approximately twice that observed in cases where the tumors were unifocal. Multifocality was found to be an independent risk factor for lymph node metastasis, a result that aligns with those of Song et al. [22] and Xue et al. [19]. In this study, the probability of SLN metastasis was 10.3% (3/29), 31.6% (220/606), and 48.4% (136/281) in MRI-BIRADS classifications 3, 4, and 5, respectively. An elevated MRI-BIRADS classification was found to be associated with an increased risk of SLN metastasis which is in accordance with previous reports [20, 23]. In comparison to the non-metastasis, yet the most suspicious level Ⅰ axillary lymph node on MRI ($0.98 \pm 0.174 \times 10^{-3}$ mm^2/s), the median ADC values for metastasis ones were considerably lower ($0.92 \pm 0.143 \times 10^{-3}$ mm^2/s). The probability of metastasis to SLN is inversely proportional to the tumor's ADC value which is consistent with previous studies [19, 24, 25]. Consistent with previous research [26–28], the long axis, short axis, and cortical thickness of the metastasis lymph node were found to be substantially longer than those of the non-metastasis lymph node, as determined by univariable logistic regression.

The nomogram serves as a foundation for individualized prediction of SLN metastasis risk and demonstrates an AUC of 0.847, indicating excellent discriminatory ability. Calibration curves validated the agreement between predicted and observed probabilities, while decision curve analysis confirmed the model's clinical utility. Furthermore, a recursive partitioning analysis was used to classify patients into low-, intermediate-, and high-risk groups based on cortical thickness and ADC values.

The findings suggest that patients in the low-risk group, characterized by a cortical thickness ≤ 2.7 mm, may potentially be exempted from SLNB due to their minimal clinical risk. However, further multicenter clinical studies with larger cohorts are necessary to validate these results

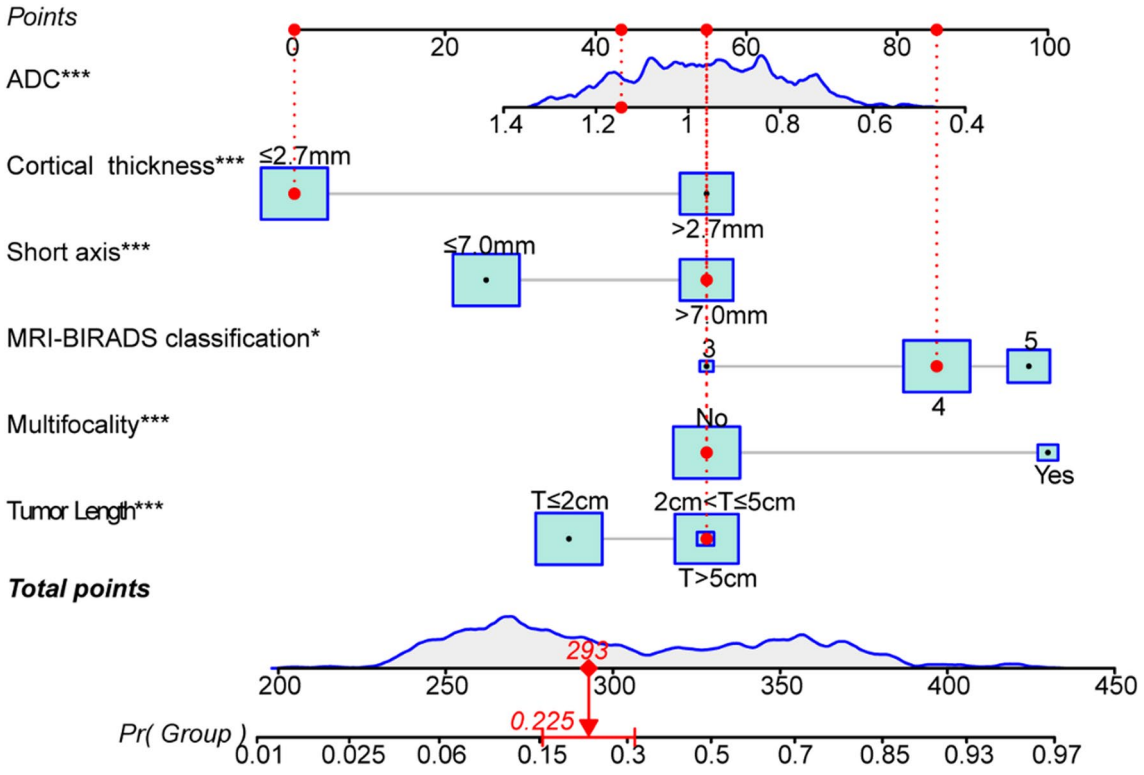

Fig. 4 Nomogram for predicting metastasis of SLN. Different variable values correspond to the scoring coordinates above, and different score values of each variable are obtained. The sum of scores of all variables is the total score, and the SLN metastasis probability of each patient can be predicted according to the corresponding metastasis probability. The unit of measurement for ADC is $10^{-3}mm^2/s$. ADC, apparent diffusion coefficient; SLN, sentinel lymph node; MRI, magnetic resonance imaging

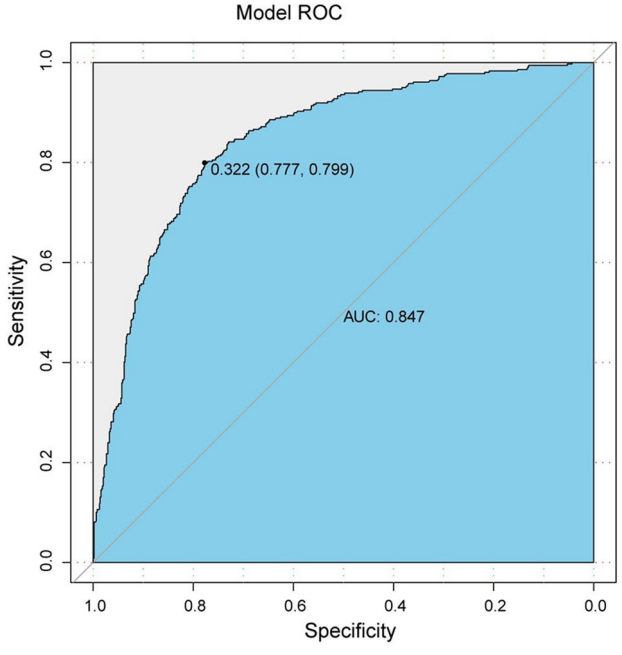

Fig. 5 Model ROC curve to evaluate the ability of model to identify SLN metastasis

and ascertain the feasibility of omitting SLNB in selected patient populations.

Although axillary ultrasound is commonly used to assess lymph node morphology preoperatively, its diagnostic performance is operator-dependent and may be limited in cases of deep-seated or multiple nodal metastases. MRI offers a more comprehensive evaluation, particularly in patients with dense breast tissue or multifocal disease. Thus, our MRI-based model may provide additional value in complex cases and institutions with access to advanced imaging modalities.

One limitation of this study is the exclusion of certain preoperative biological markers such as HER2, ER, PR, and Ki-67, which may contribute valuable prognostic information. These markers were not consistently available preoperatively in our retrospective cohort. Future prospective studies integrating imaging features with molecular and pathological data are warranted to further enhance model performance.

Furthermore, while the majority of SLNs are located at level I, where the largest lymph node was measured, there is no assurance that target lymph nodes are indeed SLNs. Due to the retrospective design, preoperative localization of lymph nodes was not performed, and therefore a direct one-to-one correlation between the lymph nodes

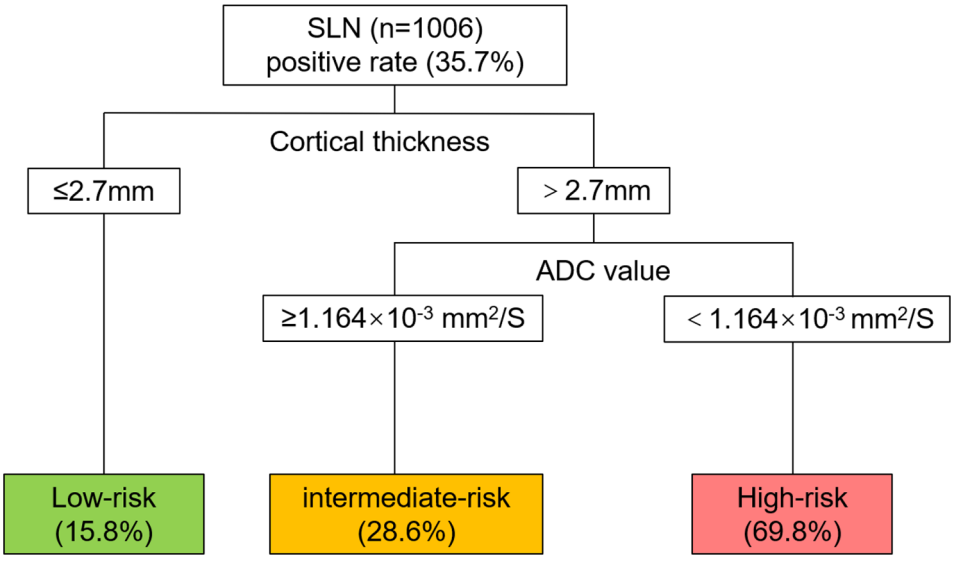

Fig. 6 Recursive partitioning analysis for risk stratification according to the probability of SLN metastasis. SLN, sentinel lymph node; ADC, apparent diffusion coefficient

measured on MRI and those evaluated in histopathology could not be confirmed. To minimize uncertainty, we endeavor to mitigate selection bias and rigorously adhere to exclusion criteria. Future prospective studies incorporating preoperative marking and intraoperative node tracking are needed to address this limitation.

Conclusion

This research examines the potential application of a decision-making model for predicting SLN involvement in breast cancer patients. The proposed preoperative model provides a framework for stratifying risks of SLN metastasis in primary breast cancer, supporting clinicians in selecting more effective personalized treatments. Importantly, the model may help identify clinically negative patients at low risk of SLN metastasis, potentially obviating the need for SLNB and reducing unnecessary surgical interventions.

Supplementary Information

The online version contains supplementary material available at https://doi.org/10.1186/s12880-025-01890-z.

Supplementary Material 1

Author contributions

Y.F. designed the study, Y.Y., Z.W., H.W. and Y. W. collected the data and Y.Y. wrote the main manuscript text. All authors reviewed the manuscript.

Funding

This research did not receive any specific grant from funding agencies in the public, commercial, or not-for-profit sectors.

Data availability

Data supporting the findings of this study are not publicly available due to restrictions related to Department of Breast Surgery, The First Affiliated Hospital of Zhengzhou University data governance. Further inquiries can be directed to the corresponding author.

Declarations

Ethics approval and consent to participate

This study was performed in accordance with the Declaration of Helsinki, and approved by the Zhengzhou University Institutional Review Board (No. 2023-KY-0586). Given its retrospective design and the use of anonymized data, the requirement for informed consent was waived.

Informed consent

Given its retrospective design and the use of anonymized data, the requirement for informed consent was waived.

Consent for publication

Not applicable.

Competing interests

The authors declare no competing interests.

Received: 24 November 2024 / Accepted: 18 August 2025
Published online: 21 August 2025

References

1. Giaquinto AN, Sung H, Miller KD, Kramer JL, Newman LA, Minihan A, Jemal A, Siegel RL. Breast cancer statistics, 2022. CA Cancer J Clin. 2022;72(6):524–41.
2. Siegel RL, Miller KD, Wagle NS, Jemal A. Cancer statistics, 2023. CA Cancer J Clin. 2023;73(1):17–48.
3. Deutsch M, Land S, Begovic M, Sharif S. The incidence of arm edema in women with breast cancer randomized on the national surgical adjuvant breast and bowel project study B-04 to radical mastectomy versus total mastectomy and radiotherapy versus total mastectomy alone. Int J Radiat Oncol Biol Phys. 2008;70(4):1020–4.
4. Hidding JT, Beurskens CH, van der Wees PJ, van Laarhoven HW, Nijhuis-van DSM. Treatment related impairments in arm and shoulder in patients with breast cancer: a systematic review. PLoS One. 2014;9(5):e96748.
5. Gupta S, Kadayaprath G, Ambastha R, Shrivastava SS. False negative rate of sentinel lymph node biopsy on intraoperative frozen section in early breast cancer patients: an institutional experience. Indian J Surg Oncol. 2022;13(2):312–5.

6. Gore RM. Upper gastrointestinal tract tumours: diagnosis and staging strategies. Cancer Imaging. 2005;5(1):95–8.
7. Liu J, Wang Z, Shao H, Qu D, Liu J, Yao L. Improving CT detection sensitivity for nodal metastases in oesophageal cancer with combination of smaller size and lymph node axial ratio. Eur Radiol. 2018;28(1):188–95.
8. Kim EJ, Kim SH, Kang BJ, Choi BG, Song BJ, Choi JJ. Diagnostic value of breast MRI for predicting metastatic axillary lymph nodes in breast cancer patients: diffusion-weighted MRI and conventional MRI. Magn Reson Imaging. 2014;32(10):1230–6.
9. Zhang W, Wang S, Wang Y, Sun J, Wei H, Xue W, Dong X, Wang X. Ultrasound-based radiomics nomogram for predicting axillary lymph node metastasis in early-stage breast cancer. Radiol Med. 2024;129(2):211–21.
10. Qiu SQ, Zeng HC, Zhang F, Chen C, Huang WH, Pleijhuis RG, Wu JD, van Dam GM, Zhang GJ. A nomogram to predict the probability of axillary lymph node metastasis in early breast cancer patients with positive axillary ultrasound. Sci Rep. 2016;6:21196.
11. Yuan C, Xu G, Zhan X, Xie M, Luo M, She L, Xue Y. Molybdenum target mammography-based prediction model for metastasis of axillary sentinel lymph node in early-stage breast cancer. Med (Baltim). 2023;102(42):e35672.
12. Zhang H, Zhao T, Zhang S, Sun J, Zhang F, Li X, Ni X. Prediction of axillary lymph node metastatic load of breast cancer based on ultrasound deep learning radiomics nomogram. Technol Cancer Res Treat. 2023;22:2071059190.
13. Zhang H, Cao W, Liu L, Meng Z, Sun N, Meng Y, Fei J. Noninvasive prediction of node-positive breast cancer response to presurgical neoadjuvant chemotherapy therapy based on machine learning of axillary lymph node ultrasound. J Transl Med. 2023;21(1):337.
14. Han P, Yang H, Liu M, Cheng L, Wang S, Tong F, Liu P, Zhou B, Cao Y, Liu H, et al. Lymph node predictive model with in vitro ultrasound features for breast cancer lymph node metastasis. Ultrasound Med Biol. 2020;46(6):1395–402.
15. Takada M, Sugimoto M, Naito Y, Moon HG, Han W, Noh DY, Kondo M, Kuroi K, Sasano H, Inamoto T, et al. Prediction of axillary lymph node metastasis in primary breast cancer patients using a decision tree-based model. BMC Med Inf Decis Mak. 2012;12:54.
16. Liu Z, Ni S, Yang C, Sun W, Huang D, Su H, Shu J, Qin N. Axillary lymph node metastasis prediction by contrast-enhanced computed tomography images for breast cancer patients based on deep learning. Comput Biol Med. 2021;136:104715.
17. Yang L, Gu Y, Wang B, Sun M, Zhang L, Shi L, Wang Y, Zhang Z, Yin Y. A multivariable model of ultrasound and clinicopathological features for predicting axillary nodal burden of breast cancer: potential to prevent unnecessary axillary lymph node dissection. BMC Cancer. 2023;23(1):1264.
18. Li X, Yang L, Jiao X. Deep learning-based multiomics integration model for predicting axillary lymph node metastasis in breast cancer. Future Oncol. 2023;19(20):1429–38.
19. Xue M, Che S, Tian Y, Xie L, Huang L, Zhao L, Guo N, Li J. Nomogram based on breast MRI and clinicopathologic features for predicting axillary lymph node metastasis in patients with Early-Stage invasive breast cancer: a retrospective study. Clin Breast Cancer. 2022;22(4):e428–37.
20. Yiming A, Wubulikasimu M, Yusuying N. Analysis on factors behind sentinel lymph node metastasis in breast cancer by color ultrasonography, molybdenum target, and pathological detection. World J Surg Oncol. 2022;20(1):72.
21. Li B, Zhao X, Wang Q, Jing H, Shao H, Zhang L, Cheng W. Prediction of high nodal burden in invasive breast cancer by quantitative shear wave elastography. Quant Imaging Med Surg. 2022;12(2):1336–47.
22. Song D, Yang F, Zhang Y, Guo Y, Qu Y, Zhang X, Zhu Y, Cui S. Dynamic contrast-enhanced MRI radiomics nomogram for predicting axillary lymph node metastasis in breast cancer. Cancer Imaging. 2022;22(1):17.
23. Zhang H, Dong Y, Jia X, Zhang J, Li Z, Chuan Z, Xu Y, Hu B, Huang Y, Chang C, et al. Comprehensive risk system based on shear wave elastography and BI-RADS categories in assessing axillary lymph node metastasis of invasive breast cancer-a multicenter study. Front Oncol. 2022;12:830910.
24. Guvenc I, Akay S, Ince S, Yildiz R, Kilbas Z, Oysul FG, Tasar M. Apparent diffusion coefficient value in invasive ductal carcinoma at 3.0 tesla: is it correlated with prognostic factors? Br J Radiol. 2016;89(1060):20150614.
25. Kim JY, Seo HB, Park S, Moon JI, Lee JW, Lee NK, Lee SW, Bae YT. Early-stage invasive ductal carcinoma: association of tumor apparent diffusion coefficient values with axillary lymph node metastasis. Eur J Radiol. 2015;84(11):2137–43.
26. Ou X, Zhu J, Qu Y, Wang C, Wang B, Xu X, Wang Y, Wen H, Ma A, Liu X, et al. Imaging features of Sentinel lymph node mapped by multidetector-row computed tomography lymphography in predicting axillary lymph node metastasis. BMC Med Imaging. 2021;21(1):193.
27. Zhang G, Li Y, Wang Q, Zheng H, Yuan L, Gao Z, Li J, Li X, Zhao S. Development of a prediction model for the risk of recurrent laryngeal nerve lymph node metastasis in thoracolaparoscopic esophagectomy with cervical anastomosis. Ann Transl Med. 2021;9(12):990.
28. Nakai N, Yamaguchi T, Kinugasa Y, Shiomi A, Kagawa H, Yamakawa Y, Numata M, Furutani A, Yamaoka Y, Manabe S, et al. Diagnostic value of computed tomography (CT) and positron emission tomography (PET) for paraaortic lymph node metastasis from left-sided colon and rectal cancer. Asian J Surg. 2020;43(6):676–82.

Publisher's note